Fabrication and characterization of bioactive glass coatings produced by the ion beam sputter deposition technique

C. X. WANG[1,2*], Z. Q. CHEN[1], M. WANG[2]
[1]Department of Dental Materials, College of Stomatology, West China University of Medical Sciences, Chengdu 610041, Sichuan, China
[2]School of Mechanical and Production Engineering, Nanyang Technological University, Nanyang Avenue, Singapore 639798, Singapore
E-mail: mcxwang@ntu.edu.sg

Ion beam sputtering and ion beam sputtering/mixing deposition techniques were used to produce thin bioactive glass coatings on titanium substrate. It was found that as-deposited coatings were amorphous. Scanning electron microscopical examination showed that the coatings had a uniform and dense structure and that fabrication parameters affected the surface morphology of the coatings. The surface Ca/P ratio of the coatings, which varied from 5.9 to 8.6 according to semi-quantitative EDX analyses, was correlated with the fabrication condition. Depth profiling of the coatings revealed four distinct zones: the top surface, the thin coating zone, the intermixed zone of coating and substrate, and the substrate. Scratch tests showed that the coatings adhered well to the substrate.

1. Introduction

It was found in the 1960s that some phosphate-containing glasses could bond to bone and soft tissues, exhibiting high bioactivity [1]. The most important developments in the area of bioactive glasses have been reviewed by Hench [2]. Due to their relatively low mechanical strength and stiffness, Bioglass® (i.e. a family of bioactive glasses which contain SiO_2, Na_2O, CaO and P_2O_5 in specific proportions) and similar bioactive glasses are used only in non- or low-load-bearing applications [3].

The use of different techniques to coat metallic implants with calcium phosphate-based biomaterials has been explored in the past few decades, with the aim of combining mechanical properties of metals with the excellent bioactivity of these ceramics, which can lead to improved bonding between implants and the newly formed bone [4–6]. One of the limiting factors affecting the widespread application of bioactive ceramic coatings is the difficulties encountered in producing well-adhering coatings by an industrially feasible process. Currently, commercially available coated metal implants are manufactured by using the plasma spray technique for depositing bioactive calcium phosphate coatings. However, problems such as low bond strength between the coating and the substrate and non-uniformity across the thickness of the coating are often encountered with the plasma sprayed coatings [7]. In recent years, several other techniques, such as electrochemical deposition [8], radio-frequency magnetron sputtering [9], excimer laser deposition [10], pulsed laser deposition [11] and dipping [12], have been investigated for producing bioactive calcium phosphate coatings on metallic substrates. In addition to bioactivity, a satisfactory ceramic (or glass) coating for medical use must be dense, hard, adherent and tough [13]. Since the mid-1970s, many surface modification techniques that are based on ion implantation, such ion beam deposition (IBD) and ion beam mixing (IBM), and techniques that are based on plasma-assisted ion implantation, such as plasma source ion implantation (PSII) and plasma immersion ion implantation (PIII), have been developed rapidly and are now widely used to modify the surface of materials including metals, ceramics, and polymers [14]. Ion beam sputter deposition was investigated as a method to produce biocompatible ceramic coatings on metallic implants due to its many advantages which include the production of thin coatings with high density and excellent adhesion [15–17]. In this process, the ionized argon gas was used to sputter atoms from a ceramic target. The sputtered atoms built up on the metallic substrate that was placed in the path of the sputtered material.

In the current investigation, the ion beam sputtering and ion beam sputtering/mixing deposition techniques were used to produce thin bioactive glass coatings on titanium substrate. The influences of fabrication parameters on the structure and properties of resultant coatings are reported in this paper.

*Author to whom all correspondence should be addressed: School of Mechanical and Production Engineering, Nanyang Technological University, Nanyang Avenue, Singapore 639798, Singapore.

2. Materials and methods

A commercially available pure titanium substrate (plates of dimensions 20 mm × 20 mm × 1 mm) was mechanically polished and cleaned ultrasonically with acetone and alcohol. The bioactive glass used had the nominal composition of 35% SiO_2, 15% P_2O_5 and 50% CaO. Glass powder disks, which were to be used as the ion beam sputtering targets, were cold pressed following a standardized procedure.

The ion beam sputtering/mixing deposition system mainly consisted of one Kaufman ion source and one Freeman ion source, one target holder and one rotatable sample holder in the path of both ion beams (Fig. 1). The deposition chamber was evacuated to a base pressure of $2.8 \sim 3.7 \times 10^{-4}$Pa. Prior to deposition, etching substrates with 800 eV and 40 mA/cm^2 argon ions for 30 min was performed to clean the surface of titanium substrate. The energetic ion beam was produced by ionizing high purity argon gas (99.999% pure). After cleaning, the stage was rotated so that the substrates were placed in the path of the sputtered atoms. Glass coatings were produced by two different techniques: ion beam sputtering and ion beam sputtering/ion beam mixing. The sputtering deposited glass coatings were produced using an Ar^+ beam of 900 eV and 20 mA/cm^2 for 3 h, 1200 eV and 40 mA/cm^2 for 90 min, and 1500 eV and 60 mA/cm^2 for 60 min, respectively. The Ar^+ beam sputtering and Ar^+ beam mixing deposited glass coatings were made by firstly sputtering the target with the 1400 eV and 40mA/cm^2 Ar^+ beam for 90 min and then using the second Ar^+ beam of 60 KeV to homogenize the coating. The dosage of the Ar^+ mixing beam was 2×10^{15} ions/cm^2, 7×10^{15} ions/cm^2, and 2×10^{16} ions/cm^2, respectively. X-ray diffraction (XRD) was employed to analyze the structure of as-sputtered coatings. A Rigaiku D/max-τA X-ray diffractometer with CuK_α radiation at 40 KeV and 50 ~ 80 mA was used. Transmission electron microscopy (TEM) was also used to examine the microstructure of as-deposited coatings. Because of the brittle nature of thin glass coatings, it was very difficult to prepare suitable specimens for TEM examination directly from coatings with titanium substrate by using the conventional ion beam thinning technique. An alternative method was used and TEM specimens were successfully produced. Firstly, the glass coatings were deposited on KCl crystal substrates from a glass target. The coated samples were then put into a beaker containing distilled water. The glass coatings were peeled off after the dissolution of KCl crystal. The peeled off glass coatings were examined under a TEM (JEOL TEM-100CX, Japan).

The surface morphology of coatings was examined by using a scanning electron microscope (SEM, Hitachi X-650, Japan) and a scanning tunneling microscope (STM, Explorer STM/AFM, TopoMetrix Co., USA). To prevent charging, samples for SEM observations were coated with a thin layer of carbon. The elemental composition of coatings was determined by energy dispersive X-ray spectroscopy (EDX).

For the X-ray photoelectron spectroscopical (XPS) analysis, glass coating/titanium samples were mounted on stainless steel stubs using double-sided adhesive and placed in a vacuum chamber. The vacuum chamber was then evacuated to a minimum base pressure of 9×10^{-6} Pa. Using MgK_α radiation (1253.6 eV), the coated surfaces were scanned over a range of 0–1000 eV, with a pass energy of 100 eV. Relative atomic concentrations of all identified elements were computed from multi-element data using peak areas and established elemental sensitivity factors. In addition, spectra for the elements were computer curve fitted to yield the best binding-energy values. The binding energies for the elemental photoelectron peaks were corrected for charging using the adventitious carbon (C_{1s}) photoelectron peak at 284.6 eV as a reference.

In order to determine the distribution of various elements in the thin glass coatings, depth profiling was accomplished by sputter-etching the coated samples for various periods of time and hence obtaining chemical composition of the coating at different depths. Using Ar^+ ions, a differentially pumped ion gun (equivalent to ~ 10 nm/min sputtering rate) with a potential of 4 KV was used to sputter etch the samples. Analysis of the sputtered surfaces was performed until the surface of the titanium substrate was reached.

The adhesion of coatings to the substrate was evaluated by measuring the peel-off load (i.e. the detachment force) using a scanning type scratch test system.

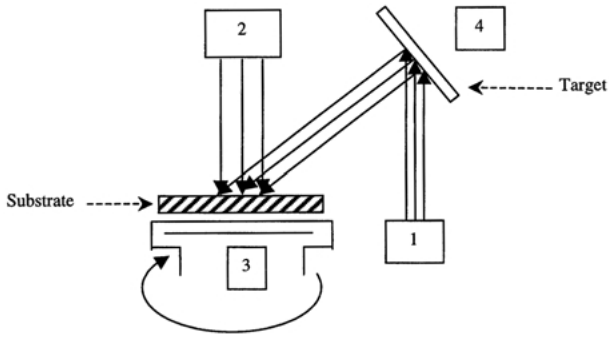

Figure 1 Schematic diagram showing the ion beam sputtering/mixing deposition technique: (1) lower energy ion source for sputtering, (2) higher energy ion source for mixing, (3) sample holder, (4) target holder.

3. Results

3.1. Structure and morphology

The XRD pattern of as-deposited glass coatings produced by ion beam sputter deposition is shown in Fig. 2. As can be seen from this pattern, the coatings only

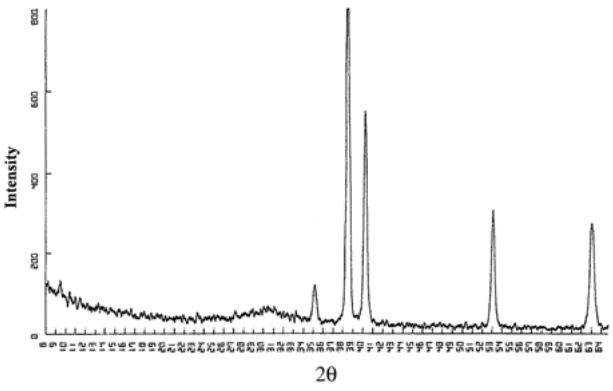

Figure 2 XRD pattern of as-deposited glass coating.

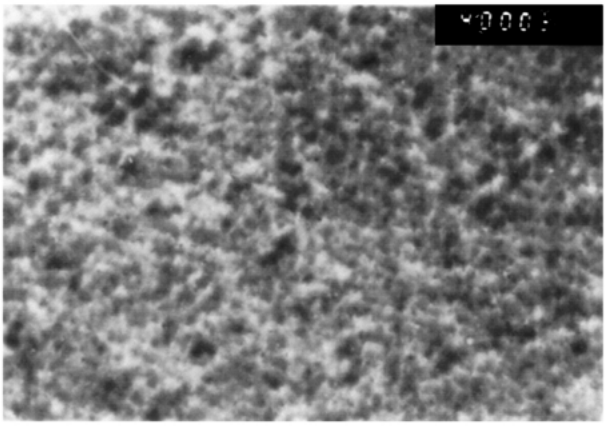

(a)

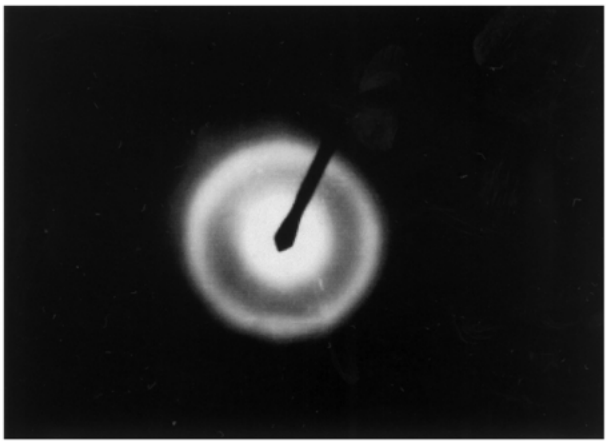

(b)

Figure 3 TEM micrograph of as-deposited glass coating on the KC1 crystal substrate: (a) bright field image, (b) corresponding selected area diffraction (SAD) pattern.

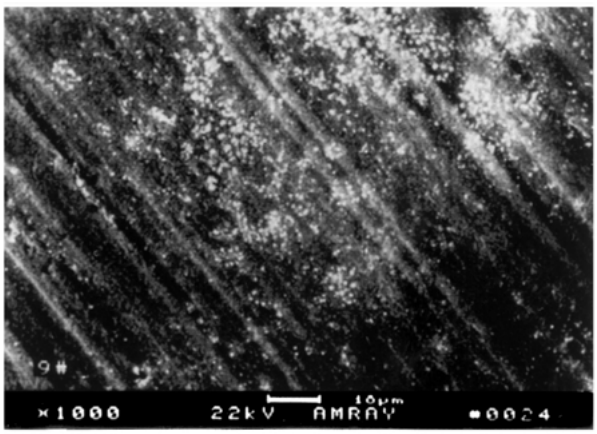

(a)

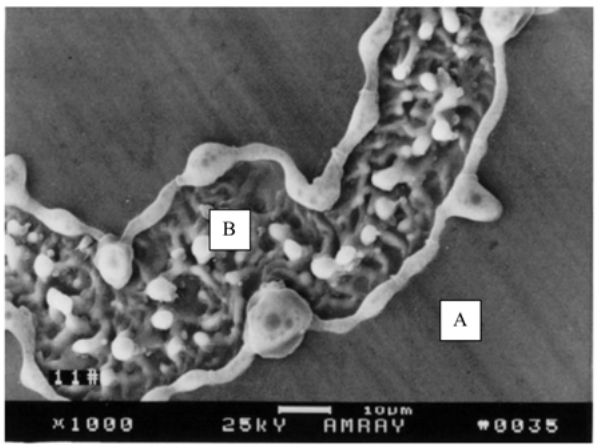

(b)

Figure 4 SEM micrographs of glass coatings deposited on titanium substrate: (a) coating produced by Ar^+ beam sputtering deposition, 1200 eV, 40 mA, (b) coating produced by Ar^+ beam sputtering and Ar^+ beam mixing process, mixing dosage 7×10^{15} ions/cm^2.

exhibited a broad hump and no peaks other than those of titanium substrate were observed, indicating that as-deposited coatings were amorphous.

The microstructure of as-deposited coatings was examined under TEM. The TEM analysis provided information on both the phases and the structure of coatings on a microscopic scale. Fig. 3(a) shows the bright field TEM micrograph of the coating deposited with the ion beam energy of 1.2 KeV and 40 mA. The corresponding selected area diffraction (SAD) pattern is shown in Fig. 3(b). A single halo in the SAD pattern indicated that the as-deposited coatings were amorphous, which confirmed XRD results.

Fig. 4 shows the surface morphology of glass coatings deposited on titanium substrate under different conditions. The surface morphology of the coating was influenced by the fabrication parameters. The coatings sputtering deposited by an Ar^+ beam of 1200 eV and 40 mA/cm^2 exhibited a clean and smooth surface morphology, while there were two different morphologies that appeared in the coatings sputtering/mixing deposited with the mixing dosage of 7×10^{15} ions/cm^2. On the surface of this coating, some areas exhibited a clean and smooth surface morphology (Area A, Fig. 4(b)), while other areas exhibited a melt-like surface morphology (Area B, Fig. 4(b)). EDX spot analysis indicated that as-deposited coatings contained calcium and phosphorous. The semi-quantitative EDX analysis of relative amounts of calcium and phosphorous revealed that the Ca/P ratio varied between 5.9 and 8.1, with the Ca/P ratio of the melt-like area being slightly higher than that of the clean and smooth area of the same coating.

Scanning tunneling microscopy (STM) is a relatively new technique for mapping a surface with high resolution. A probe can be sharpened to a few angstroms in radius at the tip and then brought to within about 2 nm above a flat surface. Piezoelectric mounts in the instrument control both lateral and up-and-down movements. This technique is based on the electron tunneling phenomenon, i.e. a current flows between the probe and the surface due to an overlap of the respective wave functions. The minute current, nanoamperes or less, varies exponentially with the tip-sample separation. The tunneling current is used to control the up-and-down movement. As the surface is scanned, a relief map (i.e. image) of the surface is obtained, with a resolution down to the atomic scale. A major advantage of STM over other imaging techniques is that the specimen does not need to be in vacuum: it can be in air or immersed in water or some other fluids. Fig. 5 shows a typical STM image of as-deposited glass coating on titanium substrate. The image gave detailed information of the

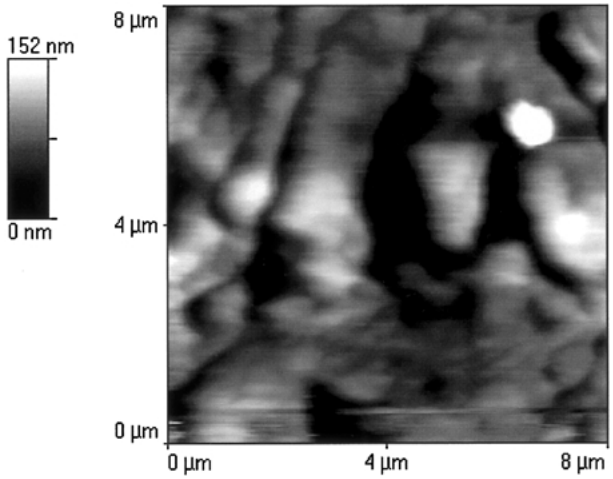

Figure 5 STM image of the glass coating produced by Ar^+ beam sputtering and Ar^+ beam mixing deposition, mixing dosage 2×10^{16} ions/cm^2.

TABLE I Binding energy of various elements obtained from the coating surface by XPS analyses

Fabrication condition	Binding energy (eV)		
	Cls	Ca2p	P2p
Sputtering, 20 mA	284.6/288.7	347.4	133.1
Sputtering, 40 mA	284.6/288.8	347.4	133.1
Sputtering, 60 mA	284.6/288.9	347.2	132.9
Mixing, 2×10^{15} ion/cm^2	284.6/288.5	347.4	133.3
Mixing, 7×10^{15} ion/cm^2	284.6/288.3	347.1	133.2
Mixing, 2×10^{16} ion/cm^2	284.6/288.7	347.1	133.3

coating surface at the atomic scale. The accumulation of sputtered atoms and formation of the coating layer are clearly shown.

3.2. Composition

XPS results obtained from the surface of glass coatings produced under different fabrication conditions are listed in Table I. It can be seen that there was no difference in the binding energy of the elements in the coatings and the sputtering target, indicating that no valence variation occurred during the deposition process. With regard to the binding energy of carbon, the binding energy at ~ 289 eV indicated the existence of CO_3^{2-}.

Fig. 6 shows the relative atomic concentration of various elements in the sputtering deposited glass coating as a function of sputter etching time. Based on these data, the coated sample could be divided into four distinct zones: the top surface, the thin glass zone, the broad glass–Ti intermixed zone, and the Ti substrate.

In the top surface which was exposed to atmosphere, large quantities of carbon were found. Beneath the top surface, there was a thin glass zone, in which no titanium element was detected. In the glass-Ti intermixed zone, glass and titanium coexisted. Under the glass-Ti zone, only Ti was present.

3.3. Adhesion

The adhesion of coatings to the substrate was evaluated using scratch tests. A scanning type scratch test system

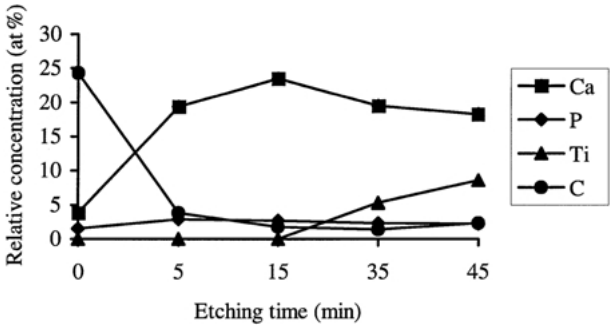

Figure 6 Compositional change in the sputtering deposited glass coating from the XPS analysis.

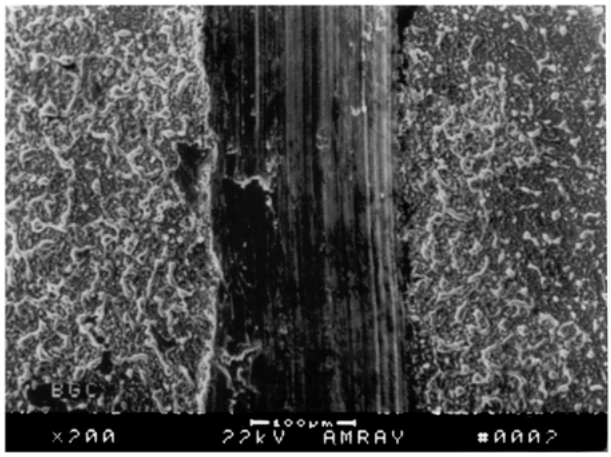

Figure 7 SEM micrograph of the scratch in the sputtering deposited glass coating.

was used, where the stylus oscillated and moved forward while being pressed on the coating-substrate system with an increasing load. The radius of the stylus was 0.1 mm, the vibration amplitude was 2 mm, and the maximum applied load was 100 gf. In the current investigation, the peel-off load could not be obtained even at the maximum applied load, indicating that the coatings were very adherent to the substrate. The scratched samples were subsequently examined under the SEM. No delamination of the coating from the substrate was observed (Fig. 7). The high adhesion strength of the glass coatings on titanium substrate may have resulted from the coating technique used.

4. Discussion

XRD and TEM analyses showed that as-deposited glass coatings were amorphous. The same observation was also made in other bioactive glass coatings produced by the plasma spray technique [18, 19]. This amorphous appearance is a direct result of the target material used and the ion beam deposition technique. This observation was verified by the STM examination, indicating that these were not nano-crystallites in the glass coatings.

The variation in the Ca/P ratio among coatings, as determined by the EDX analyzes, is attributed to the fabrication parameter used, such as sputtering energy and the mixing dosage. On the one hand, as phosphorus is very volatile, the low pressure maintained during the sputtering process affected anchoring of the sputtered phosphorus on the substrate. In addition, during the

sputtering and sputtering/mixing deposition processes, argon ions with high energy and high mixing dosage caused the loss of phosphorus atoms which led to the high Ca/P ratio. As a result, due to the loss of more phosphorus atoms in the melt-like area than in the clean and smooth area, a slightly higher Ca/P ratio was obtained in the melt-like area. According to Cotell [20], a possible cause for the high Ca/P ratio in the hydroxyapatite (HA) coating is the incorporation of carbonate group in the bioactive ceramics. The process of ion beam sputtering HA target had been studied using theoretical analysis [21]. The results showed that, because of the collision of sputtering ions and HA molecules, defects such as lattice displacement and vacancy were produced in the resultant Ca–P coating. These defects made it possible for the substitution of carbonate group for the phosphate groups in HA. The situation of Ar^+ sputtering bioactive glass target was similar to that of sputtering HA target.

As mentioned earlier, one of the advantages of using the ion beam sputtering deposition technique is the production of thin coatings with high density and excellent adhesion. The scratch tests showed that the glass coating adhered well to the titanium substrate. According to results obtained from XPS depth profiling, the glass/titanium system can be divided into four distinct zones: the top surface, the glass zone, the glass–Ti intermixed zone, and the Ti substrate. As for the composition of coatings, gradual compositional changes were achieved. During the sputtering and sputtering/mixing deposition processes, a thick glass–titanium intermixed zone was formed due to the diffusion of coating and the substrate atoms. In this zone, on the one hand, Ti atoms from the substrate were diffusing to the glass coating; on the other hand, atoms of the glass coating were also diffusing to the Ti substrate. This intermixed zone is believed to be beneficial in forming a compositional gradient. Such an intermixed zone can provide good adhesion of the deposited coatings to the substrate.

The bioactivity of sputtering deposited glass coatings was investigated using cell culture tests [22]. It was shown that the glass coatings promoted the continued growth and function of M3C3T3-E1 osteoblastic cells *in vitro*.

5. Conclusions

Dense and homogeneous bioactive glass coatings were successfully produced on titanium substrate using the ion beam deposition technique. The results showed that as-deposited coatings were amorphous. In comparison with the glass sputtering target, no valence variation of the elements in the coatings was found. Depth profiling of the coatings revealed four distinct zones: the top surface, the thin coating zone, the intermixed zone of coating and substrate, and the substrate. Scratch tests showed that the coatings adhered well to the substrate. The existence of the broad intermixed zone may have contributed to the good adhesion of coatings to the substrate.

Acknowledgments

Professor Zhong-Yang Liu and Professor Pei-Lu Wang of Sichuan University, China, are thanked for their assistance in the fabrication of bioactive glass coatings.

References

1. L. L. HENCH and H. A. PASCHALL, *J. Biomed. Mater. Res. Symp.* **4** (1973) 25–42.
2. L. L. HENCH, *J. Am. Ceram. Soc.* **74** (1991) 1487–1510.
3. L. L. HENCH and J. WILSON, (eds), ''An Introduction to Bioceramics'' (World Scientific, Singapore, 1993).
4. R. G. T. GEESINK, K. DE GROOT, C. P. A. T. KLEIN and P. SEREKIAN, *J. Bone Joint Surg.* **70B** (1988) 17–22.
5. J. BREME, Y. ZHOU and L. GROH, *Biomaterials* **16** (1995) 239–244.
6. H. DASARATHY, C. RILEY and H. D. COBLE, *J. Biomed. Mater. Res.* **27** (1993) 477–482.
7. W. R. LACEFIELD, in ''Bioceramics: Material Characteristics Versus *In Vivo* Behavior'', edited by P. Ducheyne and J. E. Lemons (Annals of the New York Academy of Science, New York, 1988) pp. 72–80.
8. H. MONMA, *J. Ceramic Soc. Japan, Int. Edition* **101** (1993) 718–720.
9. J. G. C. WOLKE, V. J. P. C. DER WAERDEN, K. DE GROOT and J. A. JANSEN, *Biomaterials* **18** (1997) 483–488.
10. R. K. SINGH, F. QIAN, V. NAGABUSHNAM, R. DAMODARAN and B. M. MOUDGIL, *ibid.* **15** (1994) 522–528.
11. C. K. WANG, J. H. LIN, C. P. JU, H. C. ONG and R. P. CHANG, *ibid.* **18** (1997) 1331–1338.
12. H. B. WEN, J. R. DE WIJIN, F. Z. CUI and K. DE GROOT, *ibid.* **19** (1998) 215–221.
13. M. WANG, X. Y. YANG, K. A. KHOR and Y. WANG, *J. Mater. Sci: Mater. Med.* **10** (1999) 269–273.
14. Q. Y. ZHANG, Z. H. LONG, C. S. REN, B. H. GUO, D. Q. XU and T. C. MA, *Surf. Coat. Technol.* **103–104** (1998) 195–199.
15. J. L. ONG, L. C. LUCAS, W. R. LACEFIELD and E. D. RIGNEY, *Biomaterials* **13** (1992) 249–254.
16. J. L. ONG and L. C. LUCAS, *ibid.* **15** (1994) 337–341.
17. C. X. WANG, Z. Q. CHEN, M. WANG, Z. Y. LIU and P. L. WANG, *J. Biomed. Mater. Res.* **55** (2001) 587–595.
18. T. KITSUGI, T. NAKAMURA, M. OKA, Y. SENAHA, T. GOTO and T. SHIBUYA, *ibid.* **30** (1996) 261–269.
19. J. A. HELSEN, J. PROOST, J. SCHROOTEN, G. TIMMERMANS, E. BRAUNS and J. VANDERSTRAETEN, *J. Eur. Ceram. Soc.* **17** (1997) 147–152.
20. M. C. COTELL, *Appl. Surf. Sci.* **69** (1993) 140–148.
21. C. X. WANG, Z. Q. CHEN and H. L. ZHANG, ''Proceedings of the 20th Annual International Conference of IEEE'', Hong Kong (1998) 2890–2892.
22. C. X. WANG, Z. Q. CHEN and M. WANG, ''Proceedings of the 10th International Conference on Biomedical Engineering'', Singapore (2000) 263–264.

Received 21 March 2000
and accepted 24 July 2001